ISSN 1063-7834, Physics of the Solid State, 2020, Vol. 62, No. 9, pp. 1604–1611. © Pleiades Publishing, Ltd., 2020.
Russian Text © The Author(s), 2020, published in Fizika Tverdogo Tela, 2020, Vol. 62, No. 9, pp. 1440–1446.

SUPERCONDUCTIVITY

Spectral Response of Arrays of Half-wave and Electrically Small Antennas with SINIS Bolometers

A. A. Gunbina[a, b, *], M. A. Tarasov[c], S. A. Lemzyakov[d, e], A. M. Chekushkin[c], R. A. Yusupov[c], D. V. Nagirnaya[c], M. A. Mansfel'd[a, b], V. F. Vdovin[a, b], D. Winkler[f], A. S. Kalaboukhov[f], S. Mahashabde[f], and V. S. Edel'man[d]

[a] *Institute of Applied Physics, Russian Academy of Sciences, Nizhny Novgorod, Russia*
[b] *Alekseev State Technical University, Nizhny Novgorod, Russia*
[c] *Kotelnikov Institute of Radio Engineering and Electronics, Russian Academy of Sciences, Moscow, Russia*
[d] *Kapitza Institute for Physical Problems, Russian Academy of Sciences, Moscow, Russia*
[e] *Moscow Institute of Physics and Technology, Dolgoprudny, Moscow oblast, Russia*
[f] *Chalmers University of Technology, Göteborg, Sweden*
**e-mail: aleksandragunbina@mail.ru*

Received March 26, 2020; revised March 26, 2020; accepted April 2, 2020

Abstract—Two types arrays of annular half-wave and electrically small antennas with typical sizes of the elements corresponding to 1/10 of the wavelength at SubTHz band with integrated superconductor–insulator–normal metal–insulator–superconductor (SINIS) bolometers have been developed, fabricated and experimentally studied. We performed numerical modeling of the full structure and use additional reference channels in experimental studies to enhance the accuracy of the spectral response estimations of receiving arrays. In experiments three reference channels were used for normalization of the spectral response: a pyroelectric detector outside the cryostat, and two cold channels—a RuO_2 bolometer and on-chip thermometer comprising series array of NIS-junctions.

Keywords: SINIS-bolometers, arrays of planar antennas, terahertz radiation
DOI: 10.1134/S1063783420090097

1. INTRODUCTION

Astronomic observations in the millimeter and submillimeter bands [1] become topical over recent years, there have appeared a demand in high sensitive receiving systems based on cooled bolometers. Such systems have contradictory requirements: the noise equivalent power (NEP) should be at least 10^{-16} W/Hz$^{1/2}$ for ground-based and by three orders of magnitude better for space observatories with a wide dynamic range for operation under conditions of a relatively high background power (tens of pW for ground-based observatories). At present time the most advanced and widely used types are transition edge sensors (TES) [2, 3] and kinetic inductance detectors (KID) [4, 5]. TES have high sensitivity, but their dynamic range is narrow, rate is low, and operation requires high stability of the bath temperature. The main advantage of KIDs is a low level of intrinsic noise due to the absence of the Nyquist noise, but the absolute value of the kinetic inductance response is low. In the superconductor–insulator–normal metal–insulator–superconductor (SINIS) [6, 7] bolometers presented in this study these disadvantages were overcome. A single SINIS bolometer is saturated at a power level about 1 pW. Therefore, such bolometers are connected into arrays so as to distribute the energy of the signal collected by the telescope mirror among many single bolometers. The NEP of such structures is not worse than 10^{-16} W/Hz$^{1/2}$, and it can be improved at least by an order of magnitude by improving the readout system replacing room-temperature amplifiers by cold amplifiers and using the microwave readout.

We developed and studied in a wide frequency range (60–600 GHz) two types of receiving arrays of annular antennas: the first type consists of antennas 300 μm in diameter designed to operate at a central frequency of 350 GHz as conventional half-wave antennas; and the second type consists of antennas 50–60 μm in diameter and is electrically small for this frequency (array in the metamaterial configuration). The first experimental results with arrays of "electrically small antennas" were obtained by irradiating of the half-wave 300-μm-diameter antenna array designed for a central frequency of 350 GHz at a significantly lower frequency of 60 GHz. The responsivity was quite high and the spectral response became

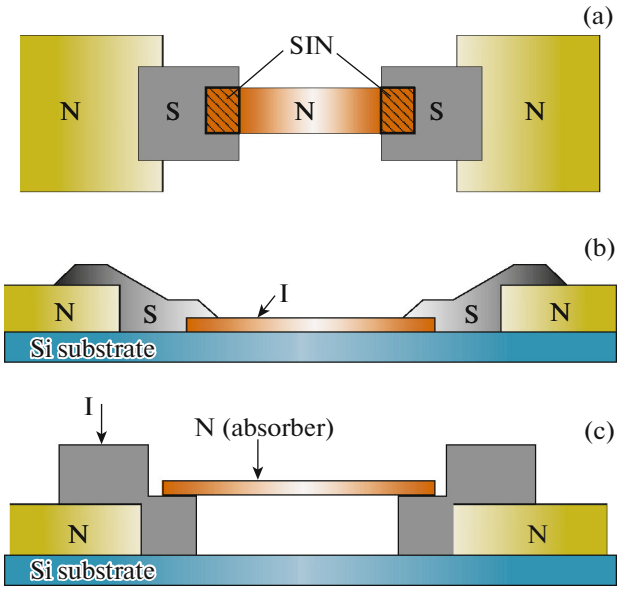

Fig. 1. Schematic image of a SINIS bolometer (N—normal metal, I—insulator, S—superconductor): (a) Top view. (b) Side view of the SINIS bolometer with the absorber on the substrate. (c) Side view of the SINIS bolometer with a suspended absorbed.

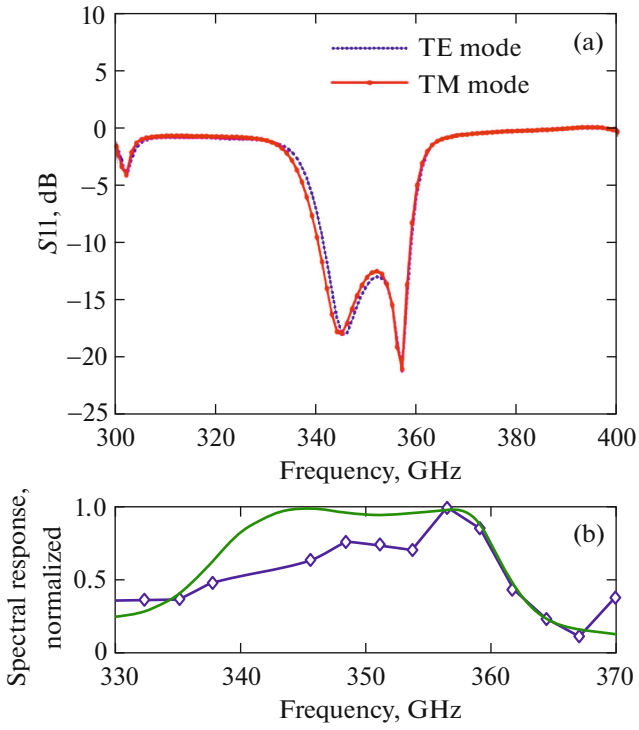

Fig. 2. *S*11-parameter (a) and spectral response (b) in the simplified case from [10]; the symbol line in (b) is the experimentally measured response.

more uniform. This led to the decision to reduce proportionally the diameter of the rings to adjust them to the signal frequency of 350 GHz, i.e., down to 50 μm. This was done in our metamaterial arrays with three types of antennas with a diameter of 50–60 μm [7].

As we have found out that it is necessary to simulate the entire structure and to use in experiments an additional calibration of the incident signal to estimate the spectral response of such arrays with a higher accuracy.

2. SINIS BOLOMETER

The sensitive element of such bolometer is the absorber made of normal metal. Two NIS junctions connected in series with an absorber serve as thermometers. Radiation absorption in the SINIS structure leads to heating of the absorber, which can be measured as the tunnel current increase in the NIS thermometers. The schematic image of a SINIS bolometer is shown in Fig. 1. The sensitivity of such bolometers can be estimated using non-equilibrium distribution functions of electrons and phonons and the theory of quantum absorption of radiation [8]. A SINIS bolometer with a suspended absorber seems to be promising way for increasing of the sensitivity compared to conventional structure with absorber on the substrate [9], see Fig. 1c.

3. ARRAYS OF HALF-WAVE ANTENNAS

In the earlier studies of arrays of half-wave annular antennas with integrated SINIS bolometers [10] operating at 350 GHz, we employed the simplest of methods: the arrays were modeled with use of periodic boundaries, and in the experimental test the received signal from the bolometer array was calibrated with the use of only one reference channel located outside the cryostat. The accuracy of such calibration would be about 50%. The modeling and measuring results in narrow frequency band obtained in [10] are shown in Fig. 2. The S11-parameter (Fig. 2a) is the reflection coefficient. We obtained the spectral dependence using the calculated S11-parameter by exciting the antenna's port. According to the reciprocity theorem, the antenna works equally to both receiving and transmission, so the obtained data can be used for estimations of the characteristics of receiving antenna.

To bring the simulation results close to real conditions it is necessary to model a full array with open boundaries. This method significantly increases the modeling time, but gives a more accurate result. At the same time, one should bear in mind that even this way of simulation will not yield a complete electrodynamics description, since under real experimental conditions there is a huge number of spatial modes and multiple reflections of the signal on the path from the source to the receiving array to be considered.

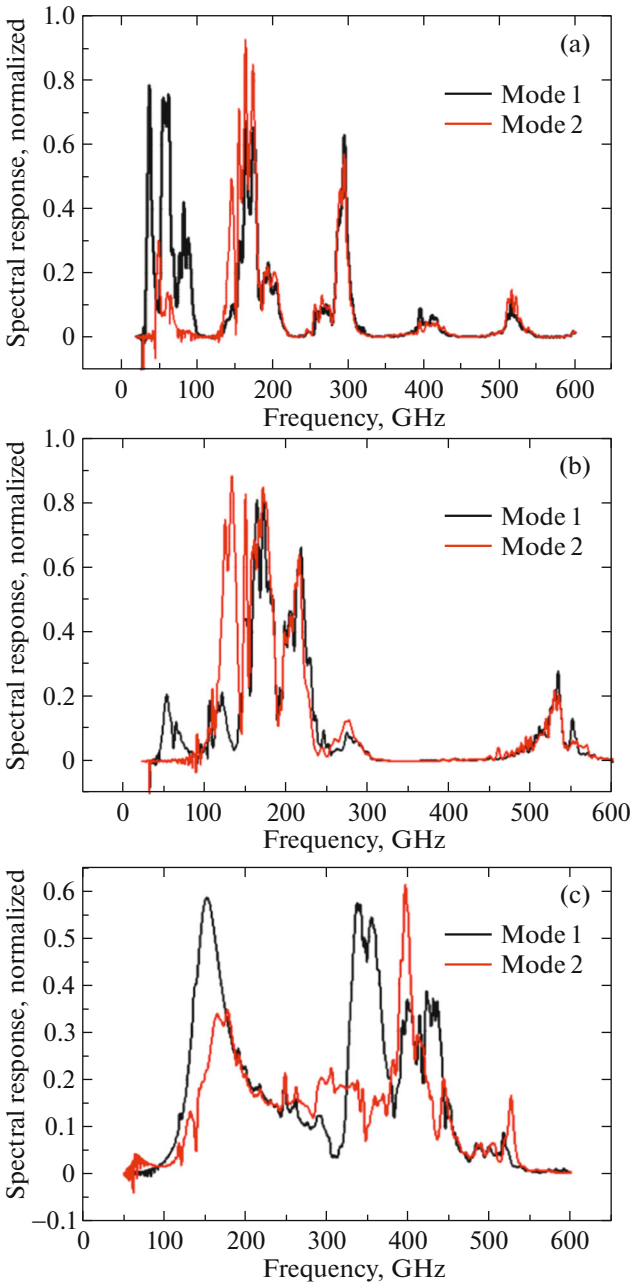

Fig. 3. The results of modeling of half-wave antenna arrays in the 350 GHz band and fabricated on substrates with different thickness: (a) 380 μm, thickness of a standard silicon substrate; (b) 127 μm, half-wave substrate; (c) 64 μm, quarter-wave substrate.

The incoming signal absorption efficiency significantly depends on the thickness of the substrate on which the array of planar antennas is fabricated. In more detail this issue was discussed in [11]. The results of modeling of the receiving array of half-wave annular antennas for three different thicknesses of the silicon substrate (permittivity 11.6): 380 μm (standard thickness), 127 μm (half-wave thickness), and 64 μm (quarter-wave thickness) are shown in Fig. 3. Mode 1 and mode 2 are orthogonal polarizations. The difference in their spectral response is accounted for by the connection wires between the elements of array. The simulations were done in the CST STUDIO SUITE software with open boundaries and circular waveguide as a guidance structure. The array consisted of 25 annular antennas with two integrated SINIS bolometers. The bolometer is presented as a serial connection of a discrete port (the resistance of the absorber 50 Ω) and a lumped element (the bolometer's NIS junction capacity is 25 fF). The elements of array can be connected in series or in parallel depending on what output resistance is required to match with the readout amplifier. In this paper we are presenting only the cases when the incoming signal irradiate the array from the antenna side, while the back side covered with 200 nm thick Ti/Au film that function as a backshort. In more detail different ways of irradiation of the receiving array (from the silicon substrate or antenna side) are discussed in [11, 12].

4. ARRAYS OF ELECTRICALLY SMALL ANTENNAS (METAMATERIALS)

An array of elements with a size and period much smaller than the wavelength (electrically small antennas) can effectively interact with electromagnetic radiation. A split ring resonator array can be a classic example of such systems [13]. For comparison, Fig. 4 shows photos of individual elements of both half-wave and electrically small annular antennas operating at 350 GHz designed by our team.

The calculation of arrays of electrically small antennas was done in three approximations. The first two simplified models were an analytical model of lumped elements and a numerical model of an infinite array with periodic boundaries for each single cell [7, 14]. The outer diameter R of the ring 54 μm and width of the ring r is 15 μm yield the inductance of the gold film $L = \mu_0 R[\ln(8R/r) - 1.75] = 54.6$ pH (μ_0 is the permeability of vacuum).

For the aluminum NIS junctions the typical specific capacity is 70 fF per 1 μm^2. For four SINIS-bolometers with eight NIS-junctions of an area of 0.8 μm^2, connected in series, we obtain a capacity of 7 fF.

From the point of view of direct current, we have two pairs of parallel-connected SINIS bolometers. But for the incoming microwave radiation, this ring is an independent elementary cell with a circular connection of four SINIS bolometers. The quality coefficient of such receiver with the typical resistance of the bolometer equal to 30 Ω will be $Q = \omega L/R = 3$, and the resonant frequency 257 GHz. Such calculation was made for the initial estimate. Numerical modeling

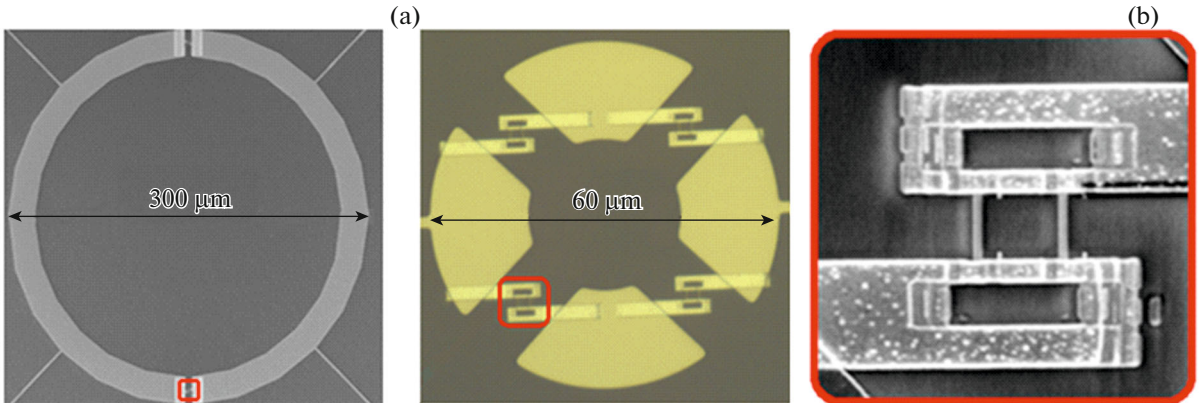

Fig. 4. Single elements of the arrays designed for 350 GHz band: (a) half-wave antenna (left) and electrically small antenna (right); (b) SINIS bolometer integrated into antennas [12].

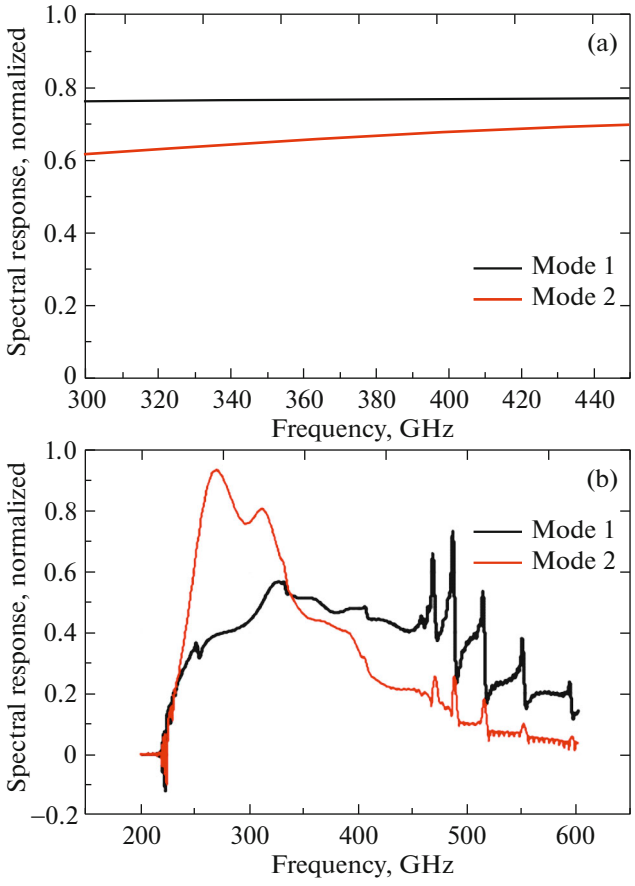

Fig. 5. The results of modeling of the electrically small antennas array: (a) Simplified model with infinite array and periodic boundary conditions, (b) modeling of full array with 100 electrically small antennas. Similar to half-wave antenna arrays, connecting wires between the elements cause the difference between modes 1 and 2. In (b), a steep decline below 220 GHz is due to the diameter of the waveguide that was used as the guidance structure.

with the use of periodic boundaries (as in [7, 14]) is only suitable for phased antenna arrays calculations. The resulting smooth curve (Fig. 5a) confirms that this approach can only be used for very preliminary approximations.

For a more realistic estimation of the spectral response, a third method was used: numerical simulation of the full structure (100 annular antennas with integrated bolometers) with open boundaries and a radiation source (waveguide port) in the far-field region. The spectral response of the system obtained in the simulation is presented in Fig. 5b.

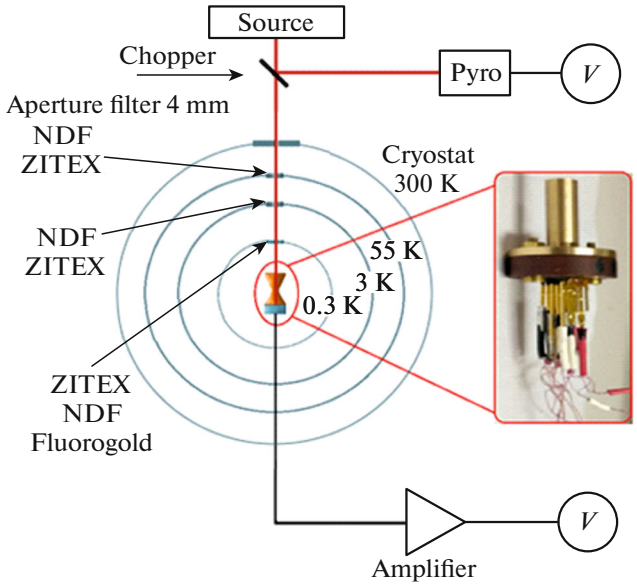

Fig. 6. The previously used experimental setup with a single reference channel located outside of the cryostat (pyroelectric detector) for measuring of the spectral response of receiving array [12].

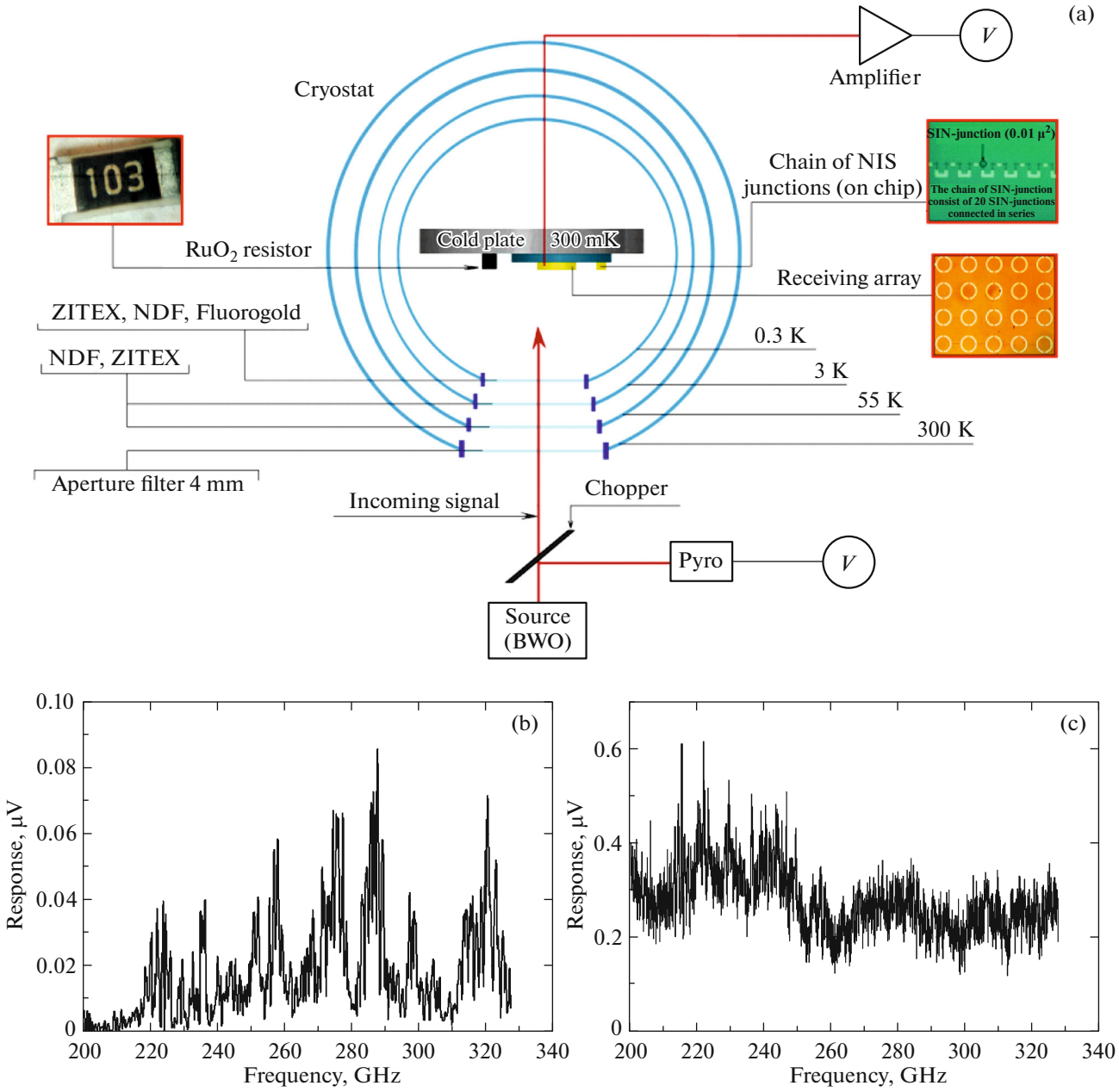

Fig. 7. Experimental setup with three reference channels: (a) Schematic view of the experimental setup; (b) reference signal measured from the ruthenium resistor; (c) reference signal measured from the on-chip chain of NIS junctions.

5. EXPERIMENTAL SETUP AND RESULTS OF MEASUREMENTS

Experimental research of the spectral response of the presented structures was done at low temperatures using the Oxford Instruments Heliox AC-V cryostat. The test sample was placed on the cold plate of the cryostat cooled down to 280 mK. The radiation source was a backward wave oscillator (BWO) operating in the range of 240–370 GHz. In the previous studies, the probe signal was calibrated with one reference channel outside of the cryostat (Fig. 6). The accuracy of such calibration does not exceed 50% as only the signal level outside the cryostat is taken into account.

This approach does not allow taking into account many multiple reflections on the cryostat windows and inside cold chamber. For improving of the accuracy of the spectral response estimation, we added two additional reference channels inside the cryostat: a ruthenium resistor [15] located on the cold plate of the cryostat near the test sample and a chain of NIS structures on the same chip as the sample under test. The experimental setup with three reference channels is shown in Fig. 7a. The reference signals measured from

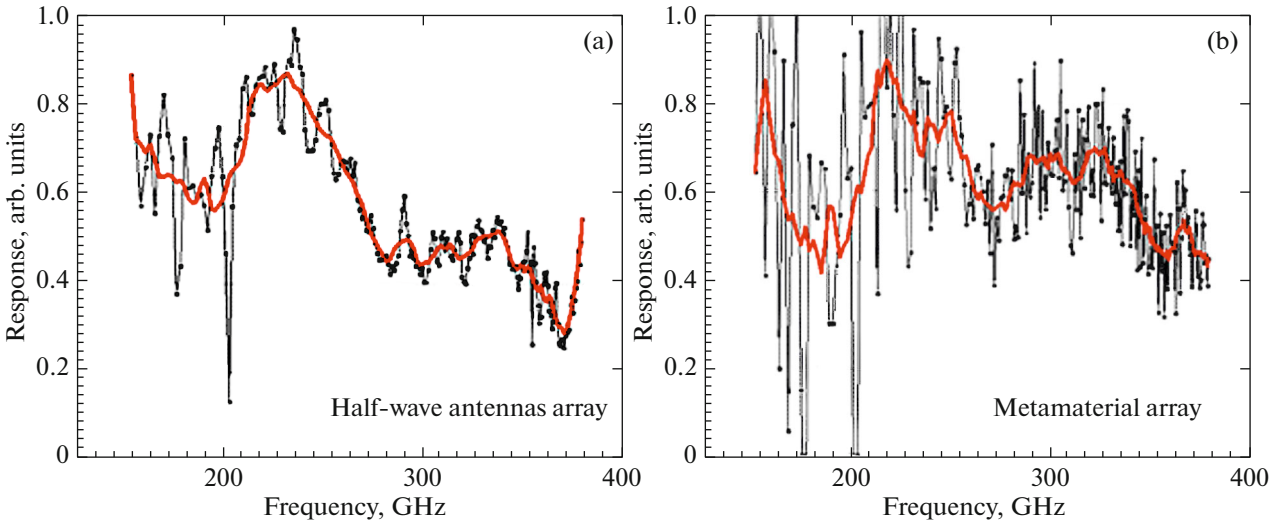

Fig. 8. Spectral response of the arrays of 350 GHz annular planar antennas normalized with the data obtained from three reference channels: (a) array of half-wave antennas, (b) array of electrically small antennas.

the ruthenium resistor and the chain of NIS junctions are shown in Figs. 7b, 7c, respectively. The measured spectral response of half-wave and electrically small antenna arrays normalized with the use of the three reference channels is shown in Fig. 8.

6. DISCUSSION

As we mentioned above, the estimation of the spectral response of the cryogenic bolometer receiving array is a challenging and complex task. Taking into account multiple reflections on the path "from source to receiver", the source signal (BWO) and with the changes of the accelerating voltage (and, accordingly, the generated frequency), the actual signal power changes significantly.

For an example, Fig. 9 shows the accelerating voltage dependence of the BWO's signal measured by the pyroelectric detector. Commercially produced BWOs are provided with calibration tables showing values of the accelerating voltage which correspond to certain values of the output signal power. However, our tests with the pyroelectric detector demonstrated that the acceleration voltage value is a very unreliable reference point for estimating the power of the incident signal. Therefore, those tables should be considered as a very rough estimate, and it is necessary to monitor it is necessary detector) while measuring the response. Further, a ruthenium resistor located on the cold plate of

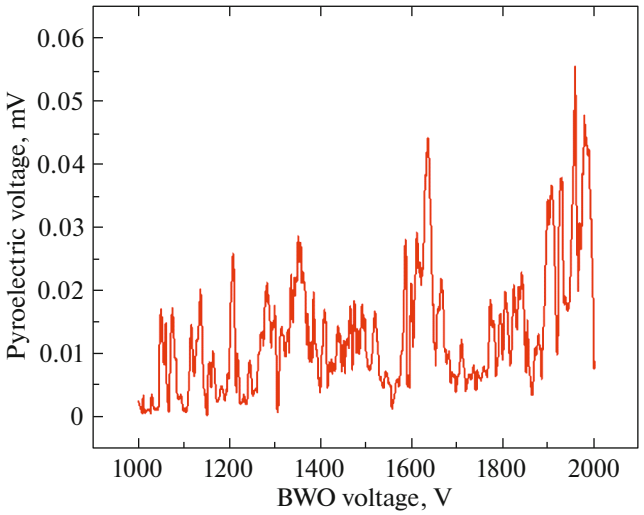

Fig. 9. Accelerating voltage dependence of the level of the BWO output signal obtained by the pyroelectric detector.

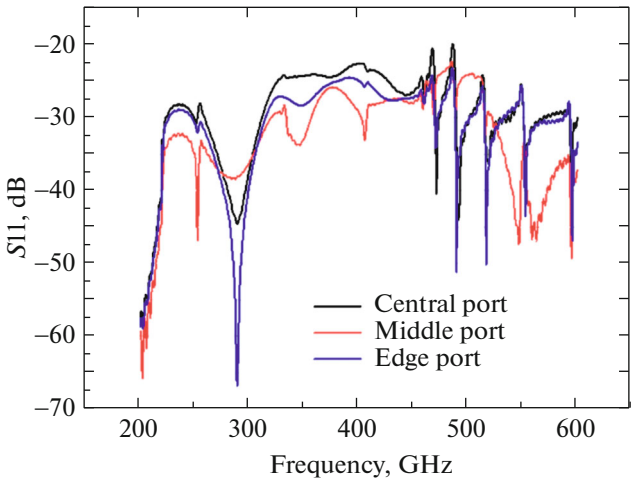

Fig. 10. *S*11-parameter of the elements of the array of electrically small antennas.

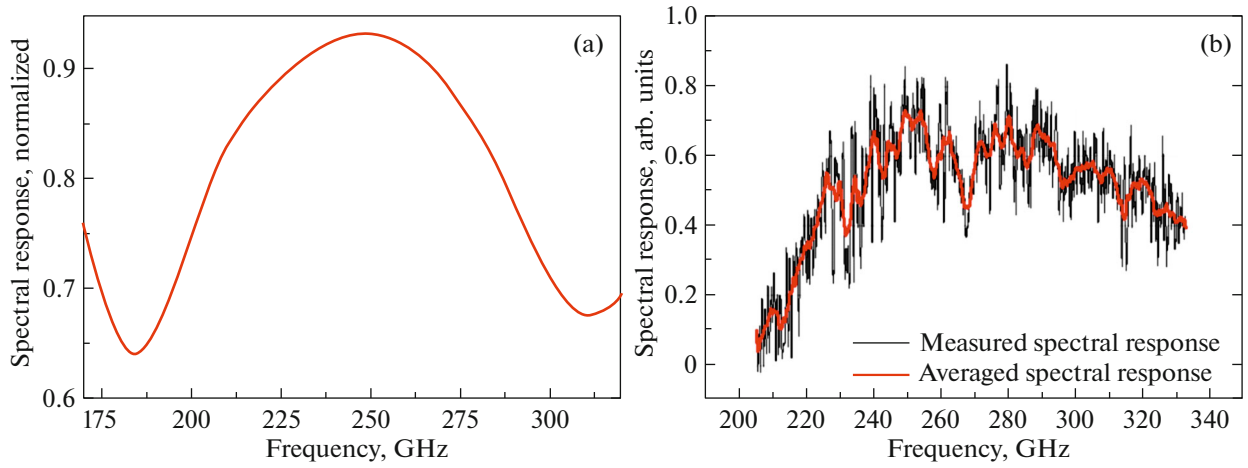

Fig. 11. Theoretically (a) and experimentally (b) [11] studied spectral response of a single annular antenna with SINIS bolometers.

the cryostat close to the test sample allows partially taking into account the reflections on the cryostat windows and inside it (Fig. 7b).

Another source of errors in this sort of tests is the thermal response of the bolometer structure as the substrate gets heated. In this case, a chain of NIS tunnel junctions located at the edge of the chip can be used as a thermometer. By registering the signal from such thermometer (Fig. 7c) and normalizing the response of the bolometric array to it, we get a more accurate estimate of the spectral response of the array.

The sources of the signal distortion listed above cannot all be simulated, because a huge processing power would be required to reproduce the path from transmitter to receiver in its entirety.

The relative unevenness of the spectral response (both in the experiment and in the simulation) is also related to the interaction of the array elements. Figure 10 shows the S11-parameter of the elements located in different places of the array of electrically small antennas. For comparison, Fig. 11 shows both the modeled and the tested response of a single ring antenna [11].

7. CONCLUSIONS

We have designed, fabricated, and experimentally studied sub-terahertz receiving arrays with integrated SINIS bolometers. The accuracy of estimation of the spectral response of the receiving array was improved by modeling a full array with all elements and using three reference channels to account for multiple reflections of the signal. The necessity of modeling a full array was confirmed experimentally by calibration with three reference channels. Modeling of a single element in an infinite array with periodic boundaries corresponds to a phased antenna array and does not describe the properties of our distributed absorber design.

FUNDING

This study was carried out as part of the state assignment of the IRE RAS (no. 0030-2019-0003) and of the IAP RAS (no. 0035-2019-0005). The manufacture and tests of the samples were done with the use of the unique research installation (USU no. 352529).

REFERENCES

1. I. I. Zinchenko, Radiofizika **46**, 641 (2003).
2. P. Day, H. G. Leduc, C. D. Dowell, R. A. Lee, A. Turner, and J. Zmuidzinas, J. Low Temp. Phys. **151**, 477 (2008).
3. B. Westbrook, A. Cukierman, A. Lee, A. Suzuki, C. Raum, and W. Holzapfel, J. Low Temp. Phys. **184**, 74 (2016).
4. P. K. Day, H. G. LeDuc, B. A. Mazin, A. Vayonakis, and J. Zmuidzinas, Nature (London, U.K.) **425**, 817 (2003).
5. S. Masi, P. de Bernardis, A. Paiella, F. Piacentini, L. Lamagna, A. Coppolecchia, P. A. R. Ade, E. S. Battistelli, M. G. Castellano, I. Colantoni, F. Columbro, G. D'Alessro, M. De Petris, S. Gordon, C. Magneville, et al., J. Cosmol. Astropart. Phys. **2019**, 003 (2019).
6. A. Tarasov, A. A. Gunbina, S. Mahashabde, R. A. Yusupov, A. M. Chekushkin, D. V. Nagirnaya, V. S. Edelman, G. V. Yakopov, and V. F. Vdovin, IEEE Trans. Appl. Supercond. **30**, 1 (2020).
7. M. Tarasov, A. Sobolev, A. Gunbina, G. Yakopov, A. Chekushkin, R. Yusupov, S. Lemzyakov, V. Vdovin, and V. Edelman, J. Appl. Phys. **125**, 1 (2019).
8. I. A. Devyatov, P. A. Krutitskii, and M. Yu. Kupriyanov, JETP Lett. **84**, 57 (2006).

9. M. Tarasov, V. Edelman, S. Mahashabde, M. Fominsky, S. Lemzyakov, A. Chekushkin, R. Yusupov, D. Winkler, and A. Yurgens, J. Phys.: Conf. Ser. **969**, 012088 (2018).

10. S. Mahashabde, A. Sobolev, A. Bengtsson, D. Andrén, M. A. Tarasov, M. Salatino, P. de Bernardis, S. Masi, and L. S. Kuzmin, IEEE Trans. Terahertz Sci. Technol. **5**, 145 (2015); S. Mahashabde, A. S. Sobolev, M. A. Tarasov, G. E. Tsydynzhapov, and L. S. Kuzmin, IEEE Trans. Terahertz Sci. Technol. **5**, 37 (2015).

11. M. A. Tarasov, A. M. Chekushkin, R. A. Yusupov, A. A. Gunbina, and V. S. Edelman, J. Commun. Technol. Electron. **65**, 60 (2020).

12. G. Yakopov, M. Tarasov, A. Gunbina, M. Mansfeld, R. Yusupov, V. Edelman, and V. Vdovin, EPJ Web Sonf. **195**, 05014 (2018).

13. R. Marques, IEEE Trans. Antennas Propag. **51**, 10 (2003).

14. A. S. Sobolev, B. Beiranvand, A. M. Chekushkin, A. V. Kudryashov, M. A. Tarasov, R. A. Yusupov, A. Gunbina, V. F. Vdovin, and V. Edelman, EPJ Web Conf. **195**, (2018).

15. S. A. Lemzyakov and V. S. Edelman, Instrum. Exp. Tech. **59**, 621 (2016).